SANDIA REPORT
SAND2002-2059
Unlimited Release
Printed July 2002

Device Technology Investigation:

Subsystems Packaging Study: Feasibility of PCSS - Based Pulser for Highly Portable Platforms

Alan Mar, Larry Bacon and Guillermo Loubriel

Prepared by
Sandia National Laboratories
Albuquerque, New Mexico 87185 and Livermore, California 94550

Sandia is a multiprogram laboratory operated by Sandia Corporation, a Lockheed Martin Company, for the United States Department of Energy under Contract DE-AC04-94AL85000.

This work was supported by Lockheed Martin Corporation under DOE Agreement number IWTA-RFL0108.

Issued by Sandia National Laboratories, operated for the United States Department of Energy by Sandia Corporation.

Available to DOE and DOE contractors from

U.S. Department of Energy
Office of Scientific and Technical Information
P.O. Box 62
Oak Ridge, TN 37831

Telephone: (865)576-8401
Facsimile: (865)576-5728
E-Mail: reports@adonis.osti.gov
Online ordering: http://www.doe.gov/bridge

Available to the public from

U.S. Department of Commerce
National Technical Information Service
5285 Port Royal Rd
Springfield, VA 22161

Telephone: (800)553-6847
Facsimile: (703)605-6900
E-Mail: orders@ntis.fedworld.gov
Online order: http://www.ntis.gov/ordering.htm

SAND2002-2059
Unlimited Release
Printed July 2002

Device Technology Investigation:

Subsystems Packaging Study: Feasibility of PCSS - based Pulser for Highly Portable Platforms

Alan Mar, Larry Bacon and Guillermo Loubriel
Directed Energy Special Applications Department
Sandia National Laboratories
P. O. Box 5800
Albuquerque, NM 87185-1153

Abstract

This report summarizes an investigation of the use of high-gain Photo-Conductive Semiconductor Switch (PCSS) technology for a deployable impulse source. This includes a discussion of viability, packaging, and antennas. High gain GaAs PCSS-based designs offer potential advantages in terms of compactness, repetition rate, and cost.

Intentionally Left Blank

CONTENTS

Section

Intentionally Left Blank

1. INTRODUCTION

Compact, lightweight, and highly efficient RF sources are of great interest for the purposes of jamming and/or damaging communications assets of an adversary using highly portable platforms. Spark gap switches are frequently used in such RF applications, but with limitations due to thermal management issues and their associated increased weight and volume, lifetime, jitter and repetition rate. This report summarizes an investigation of the use of unique Sandia-developed high-gain Photo-Conductive Semiconductor Switch (PCSS) technology for a deployable impulse source. It includes a discussion of viability, packaging, and antennas. High gain GaAs PCSS offer potential advantages in terms of compactness, repetition rate, and cost.

1.1 HIGH GAIN GaAs SWITCHES

High gain PCSS offer switching improvements in voltage, current, rise time, jitter, optical activation, size, and cost compared to other types of solid-state switch devices. Their repetition rate capability is limited by the optical trigger and charging system capabilities (up to ~MHz). They are highly compact, and can be triggered with small optical energies (<1 μJ), enabling their use with relatively inexpensive and compact laser diodes. High voltage operation of conventional (linear) PCSS is limited by optical trigger energy requirements, which are 1,000 to 100,000 times greater than those for high gain PCSS. To understand and develop high gain PCSS many experiments have been performed (for general references, see [1,2]). In order to explain what are PCSS and to describe the state-of-the-art, the following paragraphs provide a brief description of some of these associated properties and issues: (1) general device description, (2) high gain, (3) current filaments, and (4) device longevity.

1.1.1 DEVICE DESCRIPTION

The GaAs switches described in this study are lateral switches (see Figure 1.1-1) made from undoped GaAs of high resistivity $>10^7$ Ω-cm and metallic contacts that connect the switch to an energy source and a load. The simplest n contact is the ubiquitous Ni-Ge-Au-Ni-Au metallization. The p contacts are made from Au-Be. The insulating region separating the two contacts (the gap, in analogy to spark gaps) has a length that varies from 0.2 mm to 3.4 cm since higher switched voltages require a larger gap to avoid surface flashover. Because of high electric fields the switches are immersed in a dielectric liquid (Fluorinert). Pulse charging of this configuration is typically required to reduce the surface flashover problem. However, GaAs can be neutron irradiated to produce material with short (<1ns) carrier lifetime that can be used in switches that provide DC hold off and thus can be used in DC charged systems.

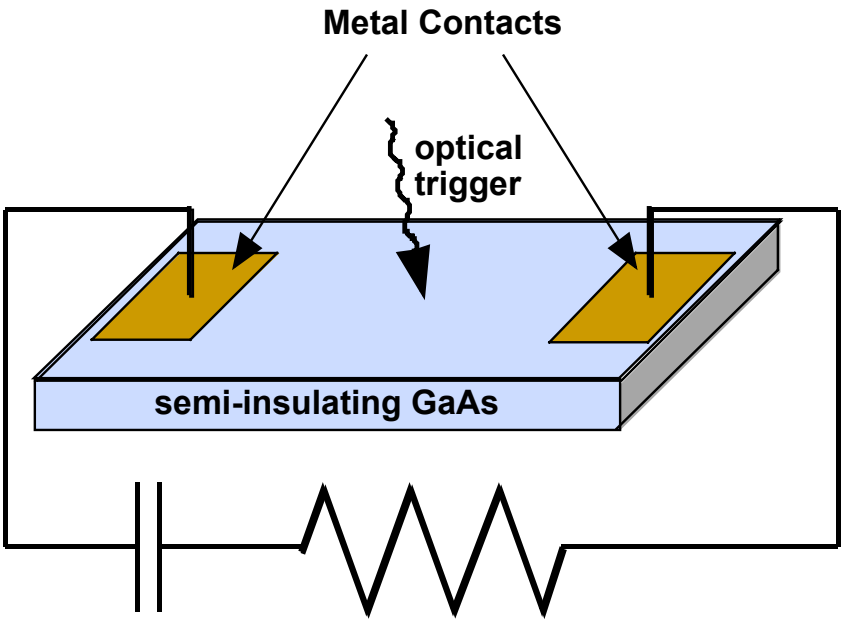

Figure 1.1-1. Schematic of the lateral semi-insulating (SI) GaAs switches used in this study. In this circuit the switch is being used to discharge a capacitor into a resistive load. The switch dimensions depend on the application. The distance between the contacts (the "gap," in analogy to spark gaps) varies from 0.2 mm to 3.4 cm, for example. Switch thickness (the vertical direction) is always 0.6 mm.

For the devices discussed in this report, laser diode arrays (LDA) are used to trigger the switch/switches (see Figure 1.1-2). Each array consists of typically four laser diodes coupled to a 300 μm-diameter fiber optic. Each array delivers about 0.7 μJ in 20 ns at about 870 nm to illuminate the switch. The wavelengths of the laser diode arrays range from 800 to 904 nm spanning the absorption band of GaAs.

Since the SNL discovery of a high gain switching mode in GaAs, these switches have been investigated for use in many high voltage applications such as: impulse and ground penetrating radar,

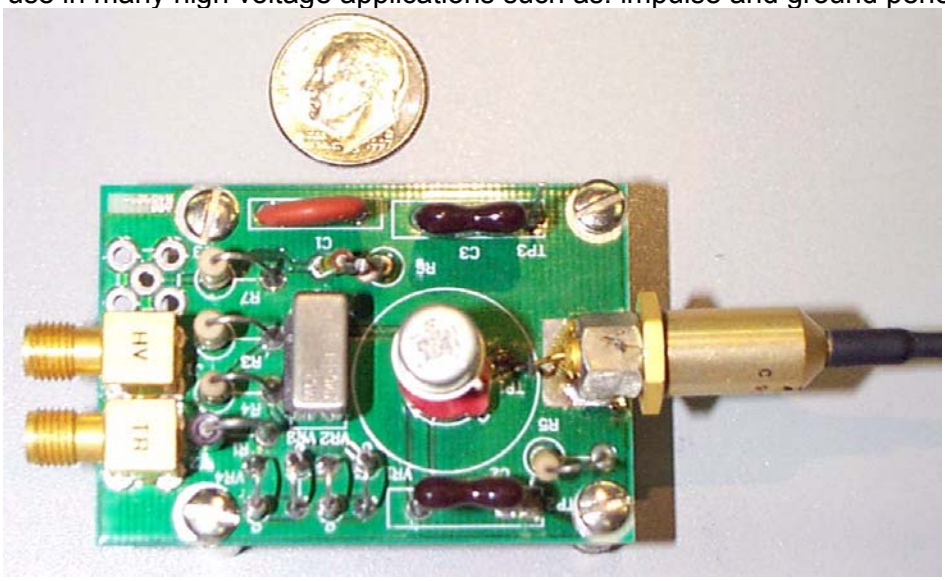

Figure 1.1-2. This close-up photograph shows the laser diode array, its electronics, and the optical fiber that directs the laser's output onto the PCSS. The laser diode is housed in the cylindrical section at the right. The connection of the optical fiber to the laser diode is barely visible at the right. To give an idea of size a dime is also shown.

switches for firing sets for weapons, as drivers for laser diode arrays to allow detection of objects through fog and smoke, and high voltage accelerators. PCSS offer improvements over existing pulsed power technology. The most significant are 100 ps risetime, kilohertz (continuous) and megahertz (burst) repetition rates, scalable or stackable to hundreds of kilovolts and tens of kiloamps, optical control and isolation, and solid-state reliability. Table I shows the best results obtained with the switches for various applications.

Table I **Parameter**	**GaAs, high gain mode, best individual results.**	**GaAs, high gain mode, simultaneous results.**
Switch Voltage (kV)	**220**	**100**
Switch Current (kA)	**7.0**	**1.26**
Peak Power (MW)	**650**	**48**
Rise time (ps)	**350**	**430**
R-M-S jitter (ps)	**50**	**150**
Optical Trigger Energy (nJ)	**2**	**180**
Optical Trigger Gain	**10^5**	**10^5**
Repetition Rate (Hz)	**1,000**	**1,000**
Electric Field (kV/cm)	**100**	**67**
Device Lifetime (# pulses)	**>100 x 10^6**	**5 x 10^4, (at 77 kV)**

Table 1.1-1. Best switching results for high gain GaAs switches. The results in the middle column are not simultaneous.

In all the applications listed, the switch has been designed as a stand-alone system with a separate laser that triggers the switch. In a separate project we demonstrated that small vertical cavity surface-emitting lasers (VCSELs), capable of being monolithically integrated with the switch, did trigger the switch. This development, coupled with recent advances in switch lifetime/longevity, will allow rapid entry into new applications.

1.1.2 HIGH GAIN

Conventional PCSS can produce only 1 electron-hole pair per absorbed photon. The energy of the individual photons excites electrons from the valence band to the conduction band. This excitation is independent of the electric field across the switch, and conventional PCSS can be operated to arbitrarily low voltage. High gain in PCSS, on the other hand, occurs only at high electric fields (greater than 4 kV/cm). The photo-excited carriers, which are produced by the optical trigger laser, gain enough energy from the electric field to impact ionize additional carriers. The additional carriers also cause impact ionization and this process results in avalanche carrier generation. Because many carriers are produced per absorbed photon, switches operating in this mode require extremely low-energy optical trigger pulses, and they are called high gain PCSS in contrast to the conventional PCSS, which are often called linear PCSS. To stand off high voltage, PCSS must be made long enough to avoid avalanche carrier generation in the absence of an optical trigger (dark breakdown). Because the optical trigger energy for a linear PCSS scales with the square of its length, high voltage linear PCSS can require rather high-energy optical trigger pulses (25 mJ for 100 kV switches switched to 1 Ω). It is the high gain feature of GaAs PCSS that allows their triggering with small semiconductor LDA. We have triggered 100 kV gallium arsenide (GaAs) PCSS, with as little as 90 nJ. A GaAs PCSS, operating in a low impedance circuit, can produce 100,000 times as many carriers as a linear PCSS would produce.

With most insulating materials (e.g. plastic, ceramic, or glass) and undoped semiconductors (e.g. silicon, gallium phosphide (GaP), or diamond), bulk avalanche carrier generation does not occur below 200 kV/cm. Semiconductors such as GaAs and indium phosphide (InP) are very different in that high

gain PCSS can be initiated at unusually low electric fields (4-6 kV/cm and 15 kV/cm, respectively). Surface breakdown limits the field across PCSS to less than the bulk breakdown field (generally 100 kV/cm). Since PCSS need to absorb light through a surface, optically activated avalanche breakdown is only practical in materials that exhibit high gain at lower fields (lower than the surface breakdown field). A very important part of the research into high gain PCSS has been to develop models for high gain at low fields in these materials.

Once avalanche carrier generation is initiated, it continues until the field across the switch drops below a threshold (4-6 kV/cm depending upon the type of GaAs). Since carrier generation causes the switch resistance to drop, in most circuits, the field across the switch will also drop. Indeed, when we first observed high gain PCSS, the most outstanding feature was that at high fields, when the switches would turn on, their voltage would drop to a constant non-zero value and stay there until the energy in the test circuit was dissipated. We originally called this switching mode "lock-on" to describe this effect. "High gain" has been adopted more recently to help distinguish this type of switching mode from other modes that also exhibit persistent conductivity, such as thermal runaway, and single or double injection. The field dependence for avalanche carrier generation that is exhibited in high gain PCSS is similar to that exhibited by Zener diodes. In series with a current limiting resistor, they will conduct whatever current is necessary to maintain a constant voltage across their contacts. In the case of a high gain PCSS, this voltage/field is the "lock-on" voltage/field or the threshold to low field avalanche carrier generation. The phase of switching during which the switch maintains this constant voltage drop is called the sustaining phase, and testing and modeling this phase is also a critical area of our research.

1.1.3 CURRENT FILAMENTS

Another important feature of high gain PCSS is that the current forms in filaments that are easily observed with a near infrared sensitive camera (most non-intensified, black and white, CCD-based cameras). When the carriers recombine (i.e. conduction electrons drop back into the valence band), infrared photons are emitted at approximately 875 nm (1.4 eV). If the filaments are near the surface of the switch, the emitted photons escape and a camera can detect them. Some images obtained in this manner are shown in Figure 1.1-3. We believe that current filaments are fundamental to high gain PCSS and we have never observed high gain without current filaments. While current filamentation can lead to catastrophic destruction of the PCSS, current amplitude and pulse widths can be limited to allow non-destructive operation. In addition, the optical trigger can be distributed across the switch in a manner that creates multiple or diffuse filaments to extend the lifetime or current carrying capacity of the switch.

1.1.4 DEVICE LONGEVITY

The biggest problem caused by the filaments is the gradual accumulation of damage at the contacts, which limits their useful life to 1-10,000,000 shots depending upon the current per filament and the optical trigger distribution. Presently, device lifetime is a limitation of this technology for some applications. PCSS degrade with use because the regions near the contacts are damaged on each pulse, and they gradually erode. The bulk semiconducting material shows very little, if any, degradation as the contact regions wear out. The fact that the degradation is confined to regions near the contacts suggests that developing better contacts that allow for higher current density can make substantial increases in switch lifetime. When this project started, high-gain PCSS would last for ~10^4 pulses under a specific set of test conditions (0.5 MW). During the course of this project, the lifetime has been improved to 100×10^6. In comparison, the semiconductor lasers, which trigger or are driven by these switches, can last from 10^8 to 10^{10} pulses.

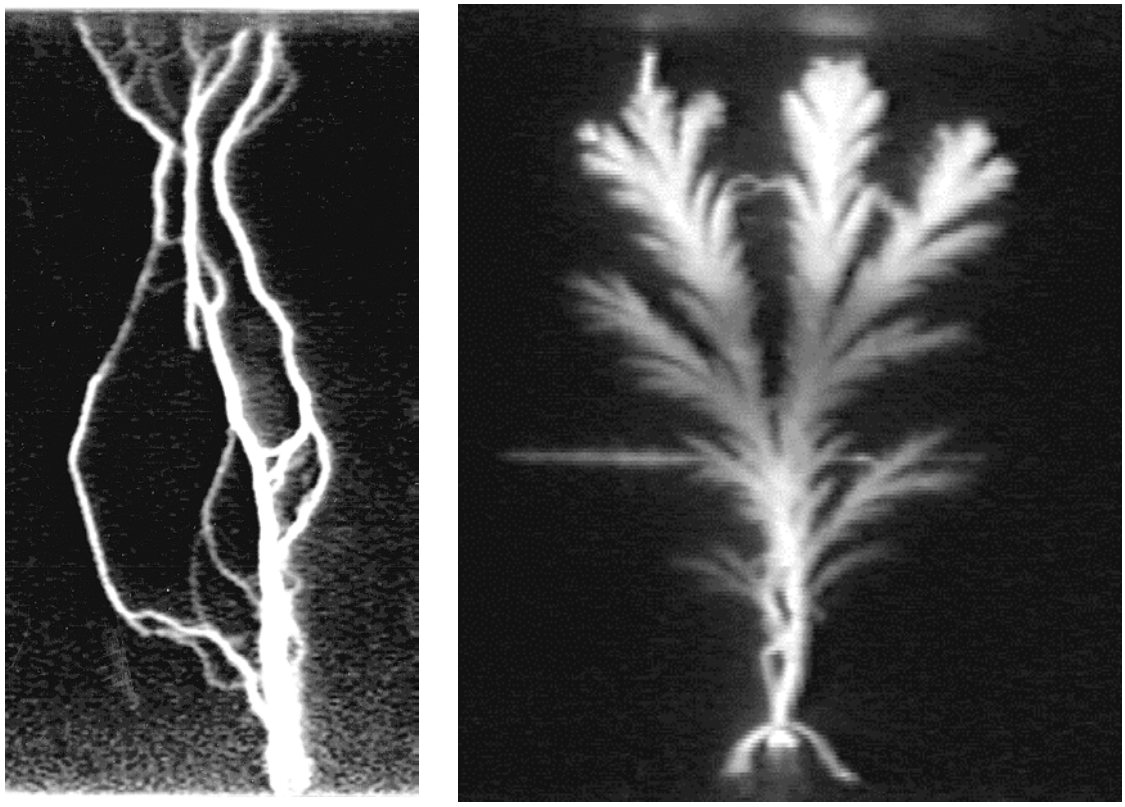

Figure 1.1-3 These photographs show examples of the current filaments that form during high gain PCSS operation. The images are recorded from the infrared (875 nm) radiation that is emitted as the carriers recombine in the switch. In both cases, the switches are 1.5 cm long (vertically). The PCSS on the left was charged to 45 kV and conducted 350 A for 10 ns. The PCSS on the right was charged to 100 kV and conducted 900 A for 1.4 ns.

Shot lifetimes of >100 million have been achieved using doped contact PCSS structures. We are presently fabricating new generations of deep-diffused and epitaxial-grown contacts that should yield further improvements. We have incorporated doped layers with high carrier concentrations under the contact regions to reduce the contact resistance and spread the current. The doped regions also serve to transfer the point of filament termination from the metal - semiconductor interface to a doped semiconductor - semiconductor interface that is more robust against damage.

Two main approaches for the fabrication of switches with doped contact layers have been developed. The first is dopant diffusion. In this process, SiN_x is deposited and patterned to serve as a diffusion mask on the GaAs. A silicon source layer and SiN_x encapsulation layer are then deposited and the Si driven in using a tube furnace at 800 °C. These layers are left in place and patterned to serve as a diffusion mask for Zn. Vaporized Zn is diffused into the substrate in an open tube furnace at approximately 600 °C. Further details regarding the diffusion processing can be found in [3]. Ohmic contacts are then made to the doped regions to complete the fabrication.

The second technique we are pursuing for doped PCSS contacts is epitaxial growth using MOCVD (metalorganic chemical vapor deposition) to incorporate grown layers of highly doped material under the contacts. In one such approach, n-type (Si-doped) material is first deposited over the entire wafer and then etched away except in the regions where the switch cathodes are formed. This process is then repeated for a p-type growth (Zn-doped) for the anodes and then ohmic contacts are made to the doped material. Because this process results in a non-planar surface, another preferred approach utilizes patterned epitaxial regrowth. In this process, the contact regions are etched to some depth (a few microns) and highly doped GaAs is then regrown into these regions by the same thickness as the etch depth using a growth mask (SiO_x) that prevents growth elsewhere. This process is also repeated

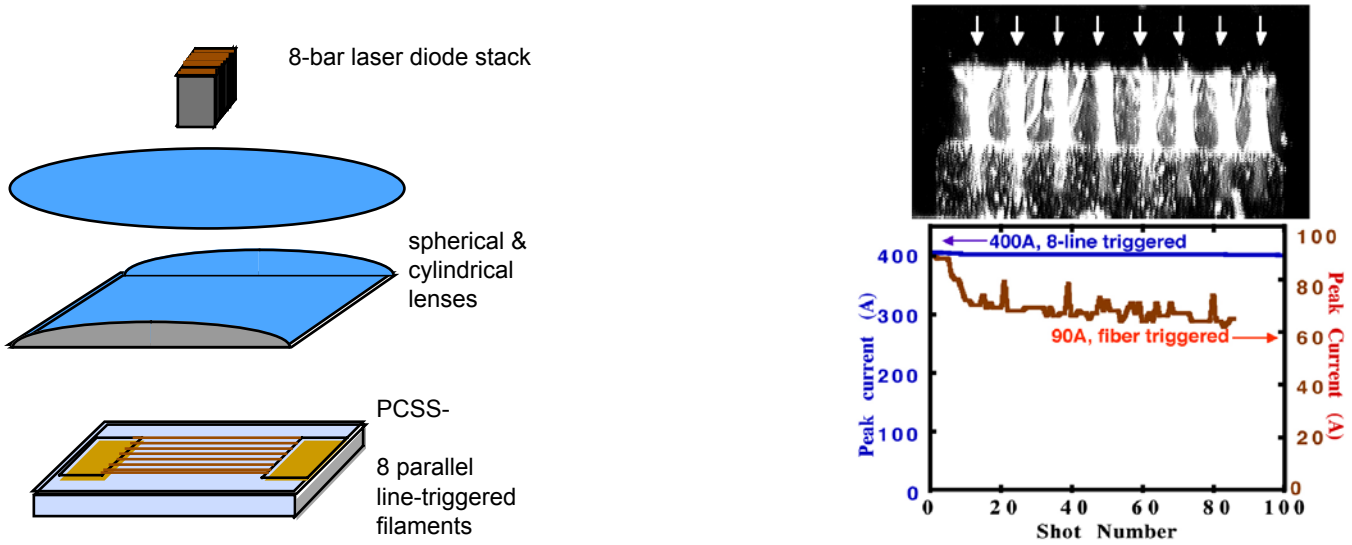

Figure 1.1-4. Multi-filament triggering of PCSS for improved longevity at high current levels.

for the two different contact polarities and ohmic contacts made to the doped layers, which results in a planar structure. Because of non-ideal behavior associated with the patterned regrowth, this process has been further refined to address the issues of conductive material grown on the growth mask (into the switch gaps), and growth non-planarity. Such switches perform very similarly to those fabricated using diffusion processing.

For longer (~100 ns) pulse durations at kA levels, the doped contact structure does not adequately suppress filament formation to prevent contact damage when a single spot trigger is used. We have addressed this regime of operation by the generation of multiple filaments using multi-line triggering. As shown in Figure 1.1-4, we have initiated 8 distinct filaments that the current will be distributed amongst. This is accomplished by near-field imaging of an 8-bar laser diode stack using an aspherical collimating lens together with a cylindrical lens. This anamorphic optical system precisely sets the magnification and aspect ratio such that the 8 laser lines exactly fill the gap length and width. When triggered in this manner, switching at nominally 400 A results in current drop of only 2% after 100 shots, with continuing switch functionality, the result of which is shown on the right in Figure 1.1-4. The same type of switch, operating at only 90 A, shows a 28% drop after 86 shots when fiber (spot) triggered, at which point complete switch failure occurs.

We have also investigated the effects on longevity of various methods of bonding to the switch contacts. The switches incorporate a gold bondpad layer on the contact surface, which is leached into solution in conventional molten Pb/Sn solder. Thus, without a solder barrier layer in the contact, Pb/Sn soldering depletes the gold at the ohmic contact interface. We therefore implemented gold ribbon thermocompression wire (ribbon) bonding or Pb/In soldering to preserve the gold bondpad layer. We found that these techniques increased the longevity by about a factor of four. Switches have now been developed that have 466 shot lifetimes at 1 kA, 100 ns.

Further lifetime improvements will be achieved through the use of interdigitated multi-gap switches that allow the generation of more filaments to achieve improved current and heat distribution in the device, without adding complexity to the optical trigger system. Such a device is shown in Figure 1.1-5, which allows the generation of 24 current filaments with the same optics used to generate 8 filaments in the single-gap structure.

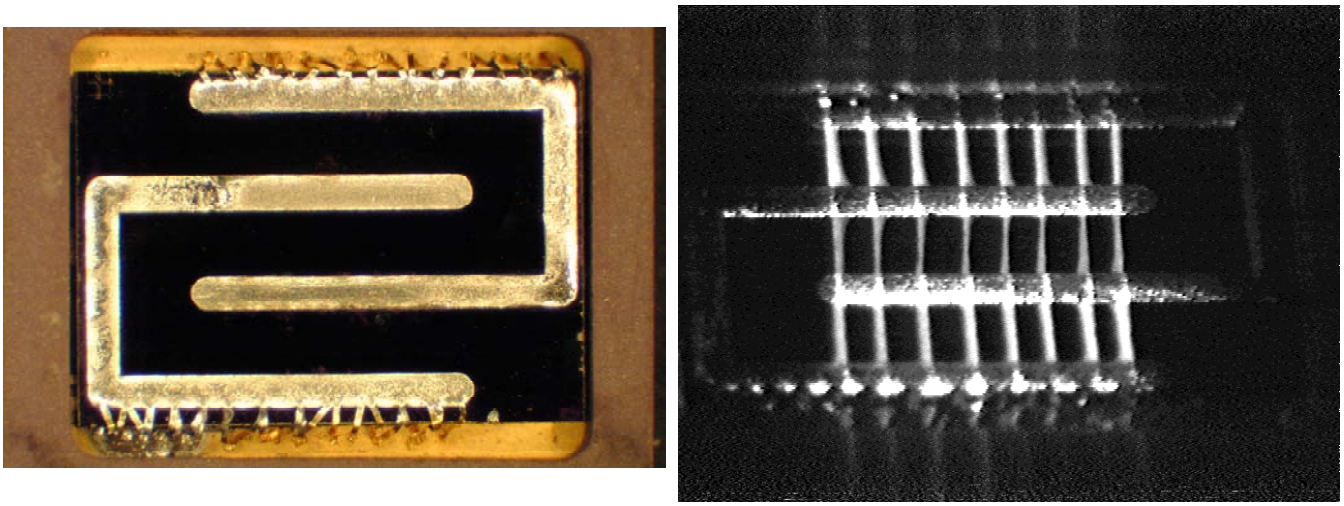

Figure 1.1-5. Interdigitated contact PCSS for multi-filament operation, shown operating at 1 kA, 100 ns.

The longevity tests have demonstrated that there is less contact degradation with short duration currents. In our longevity test-bed we utilize a pulse charger that charges a transmission line to high voltage with a risetime of about 1 μs and a total pulse width of a few microseconds. If we discharge this transmission line when the charger is at full voltage, the switches will carry a current of 10 to 50 A for the length of the transmission line (3 to 30 ns, typically) and a much smaller current for a few microseconds. This long duration "recharge current" greatly reduces device life when compared to the case when the current only lasts for tens of nanoseconds. We determined this by adding isolation diodes between the pulse charger and the transmission line. When the line was charged, the isolation diodes would hold the line at high voltage. We would trigger the switches well after the pulse charger finished, thus discharging only the transmission line.

1.2 LASER DIODE ARRAYS AND ELECTRONICS

We use small laser diode arrays to trigger the switches. Such arrays are available commercially. Ours were purchased from Laser Diode Inc. (Model CVD-167F) and consisted of an array of four or more laser diodes that are hard coupled to a fiber optic. Their wavelength is around 850 nm. Previous studies at Sandia Labs show that this is the best wavelength to use in terms of the sensitivity of the switches to this light. The pulse duration was ~13 ns. Figure 1.2-1 shows the laser pulse intensity as a function of time. The total laser energy in each pulse is measured to be about 0.65 μJ at the end of the 300-μm diameter fiber. The electronics that power this laser are built at SNL. In this case a single avalanche transistor is switched to deliver a pulse to the array. The package, shown in Figure 1.2-2, measures 2 in. by 2 in. by 1 in. The package requires a voltage of 400 VDC and a trigger. DC power supply and a trigger generator to provide the inputs to the package can be installed in a small enclosure. The power supply and trigger generator in this box are respectively about 3 in. by 1 in. by 1.5 in. (most of which is a DC to DC converter powered by 8 V) and 3 in. by 2 in. by 1 in. This laser can be used repetitively at up to 1 kHz. Thus, the assembled package size of a laser diode array, the electronics, the power supply, and trigger generator is less than 15 cubic in. (see Figure 1.1-2).

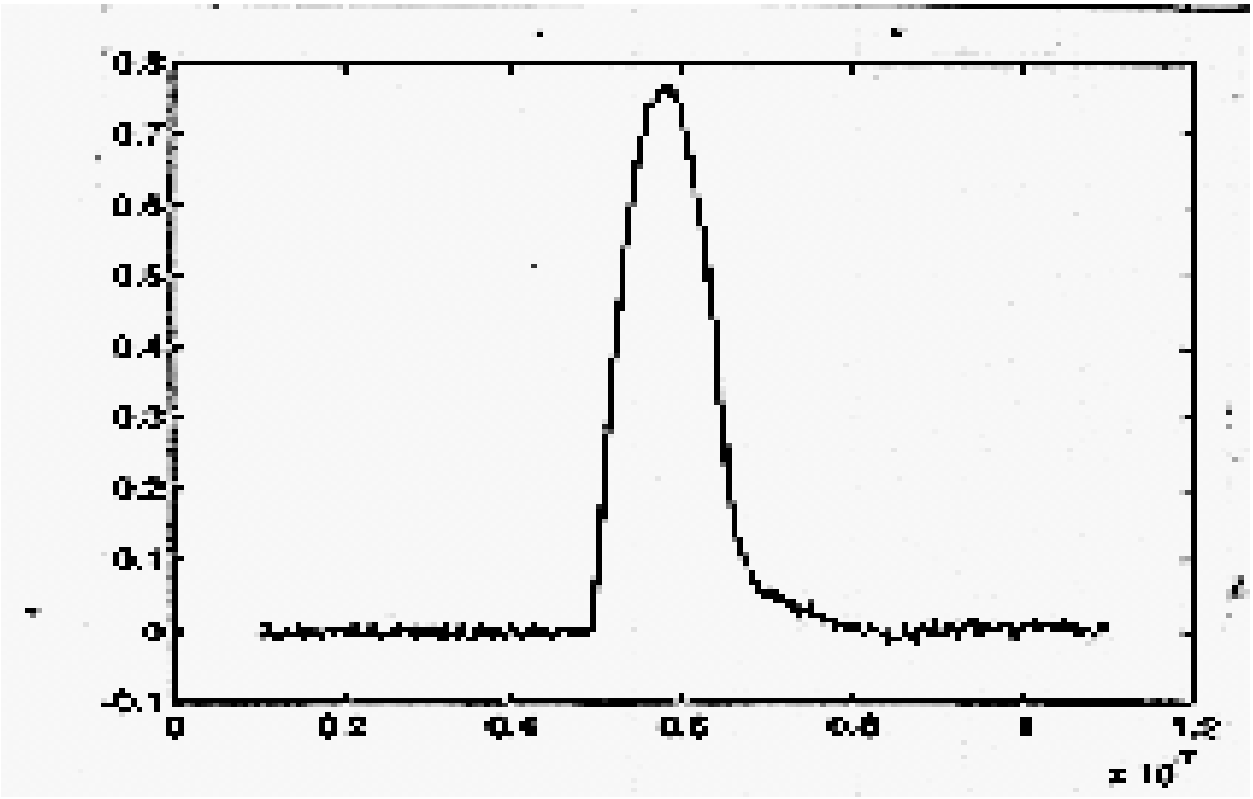

Figure 1.2-1 - The output of the laser diode array. The risetime in this waveform is 5 ns and the pulse width is 13 ns FWHM. The array's wavelength is 870 nm at 0.65 μJ per pulse.

2. RF GENERATION

2.1 L-C OSCILLATORS (LCO)

The L-C oscillator can be used with a switching element to implement a simple, highly efficient means to create RF bursts. As shown in figure 2.1-1, the switch couples the charged capacitor to the inductor, which causes a damped ringing waveform to be applied to the load. The switch is then opened to allow the capacitor to recharge, at which point the process can be repeated. For V=30 kV, C=10 pF, L=10 nH, and Rload=100 Ω, this ringing occurs at about 160 MHz.

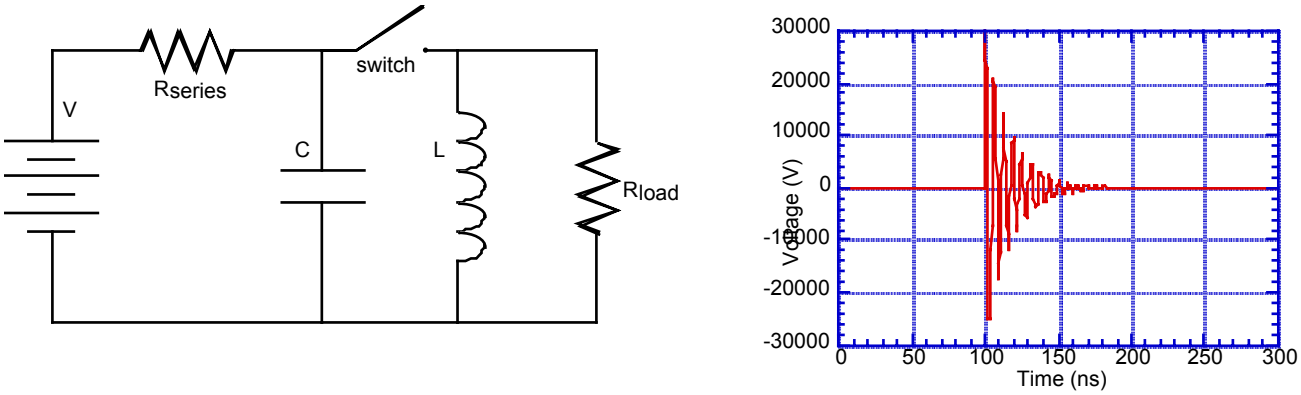

Figure 2.1-1. Switched LCO diagram and output waveform for C=10 pF, L=10 nH and Rload =100 Ω.

This behavior is for an ideal switch that has no losses. As discussed in 1.1, the PCSS switching mechanism incurs a voltage drop in the on state to maintain the lock-on field. If a PCSS is used in the switched LCO, this drop will occur on each cycle of the RF waveform, resulting in rapid damping of the RF burst. A PCSS with a 5 mm gap could be necessary to switch at 30 kV, and as much as 3 kV lock-on voltage would occur in such a device. The resulting waveform from the LCO with such a switch is shown in Figure 2.1-2:

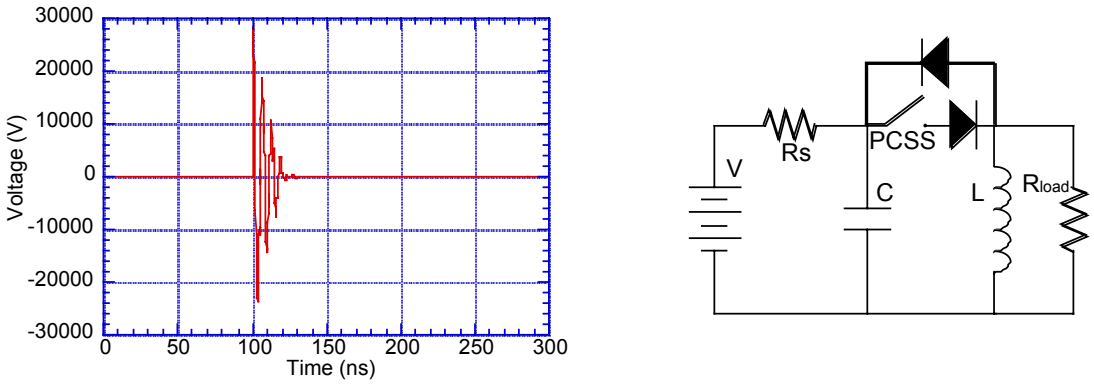

Figure 2.1-2. PCSS -switched LCO waveform showing rapid damping due to lock-on voltage losses. Reverse current and negative voltage losses can be improved by using diodes on the PCSS.

The other problem with this configuration is the reverse current in the PCSS on the negative portions of the waveform. This reverse current causes dissipation in the ohmic contacts of the PCSS, causing orders of magnitude greater contact damage than in forward bias. The problems of reverse-current and voltage loss might be partially corrected through the use of two (fast recovery) diodes, but the damping loss improvement is only marginal.

A more practical use of the PCSS to switch an LCO is shown in Figure 2.1-3. Because a conventional PCSS can hold off the high voltage for only a few μs, a modulator is used to pulse charge the system. The maximum repetition rate of the system will be determined by the limit of this modulator. Such modulators are the subject of section 2. The modulator charges a storage capacitor that is held at peak voltage through a diode. After this capacitor completes charging, the PCSS is triggered on and discharges into the primary of a coupling/step-up transformer. A rectifier diode blocks reverse current to the PCSS. The secondary of this transformer is used as the resonating L of the LCO. High peak voltages in the output compared to the primary power supply can be obtained from this configuration, as shown in Figure 2.1-4.

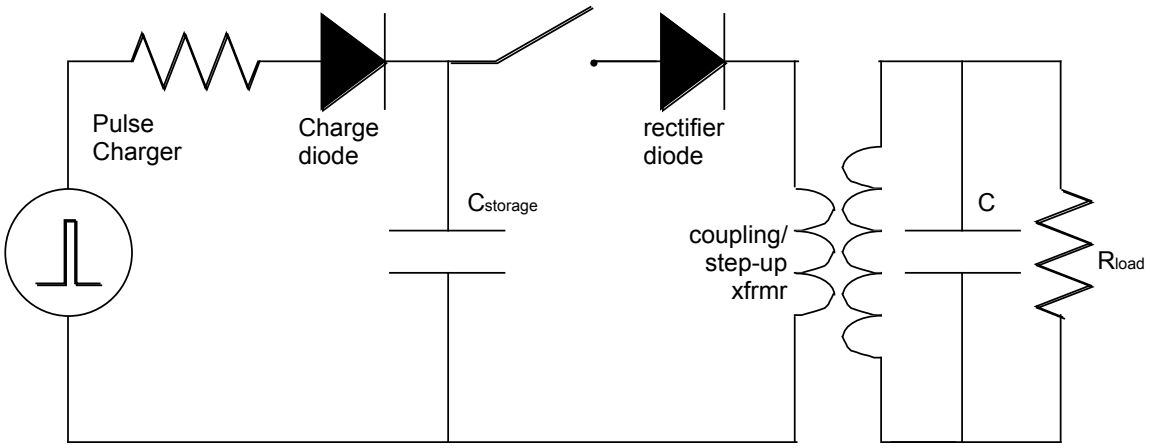

Figure 2.1-3. Pulse-charged LCO using PCSS with step-up transformer.

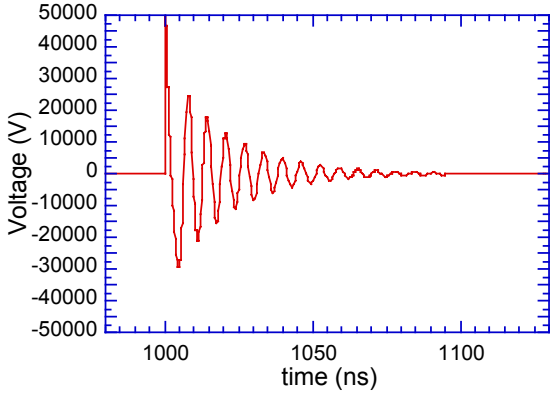

Figure 2.1-4. Output of pulse-charged LCO using PCSS with step-up transformer. $C_{storage}$=0.5 nF, $L_{primary}$=4 nH, $L_{secondary}$=10 nH, C=0.1 nF, R_{load}=100 Ω. A charge pulse similar to that in Figure 2.2-3 is assumed.

The pulse charger might be replaced with a simple DC power supply if a neutron-irradiated PCSS is used. As discussed in section 1.1.1, such a switch is capable of holding off DC high voltage. This would not only offer a size and complexity advantage, but also increase the potential repetition rate of the system. PCSS have been triggered at MHz repetition rates in burst mode [4]. The limit in this system would be due to heating in the PCSS due to lock-on and resistive losses. The lock-on loss will cause heating of the bulk GaAs, and damage associated with this loss has not been observed. Rather, contact damage has always been the limiting factor in PCSS lifetime

It is difficult to predict the lifetime of PCSS operated in this regime. About 25 μC of charge would be switched by the PCSS for each RF burst, with the peak current being nearly 40 kA for less than 0.5 ns. Fireset PCSS triggered with 8 parallel filaments have switched about 50 μC of charge with nearly 500 shot lifetime. However, ohmic heating in the contacts will scale with the square of the current. Integrating the square of the switched current, we calculate 0.66 J/Ω (dissipation for each ohm of contact resistance) for this circuit, vs. about 0.04 J/Ω in the 500 shot lifetime fireset PCSS example. Because this dissipation scales with total contact resistance, it can be reduced by using multiple parallel filaments, and by lowering the contact resistivity by doping the GaAs beneath the contacts, as discussed in 1.1-4.

Fast recovery reverse current-blocking diodes as described above with sufficient speed and power handling capability may not be available. An alternative approach may be to use two PCSS connected in parallel with opposite polarities, the intent being that the reverse-connected switch will conduct the reverse current and prevent rapid damage to the forward connected switch. Experiments need to be conducted to test this concept.

2.2 PULSE FORMING LINES

Switched pulse-forming networks could also be used to generate RF. In this section we will describe a 1.) Double switched line, 2.) a Folded line, 3.) the Frozen Wave generator.

2.2.1 DOUBLE-SWITCHED LINE

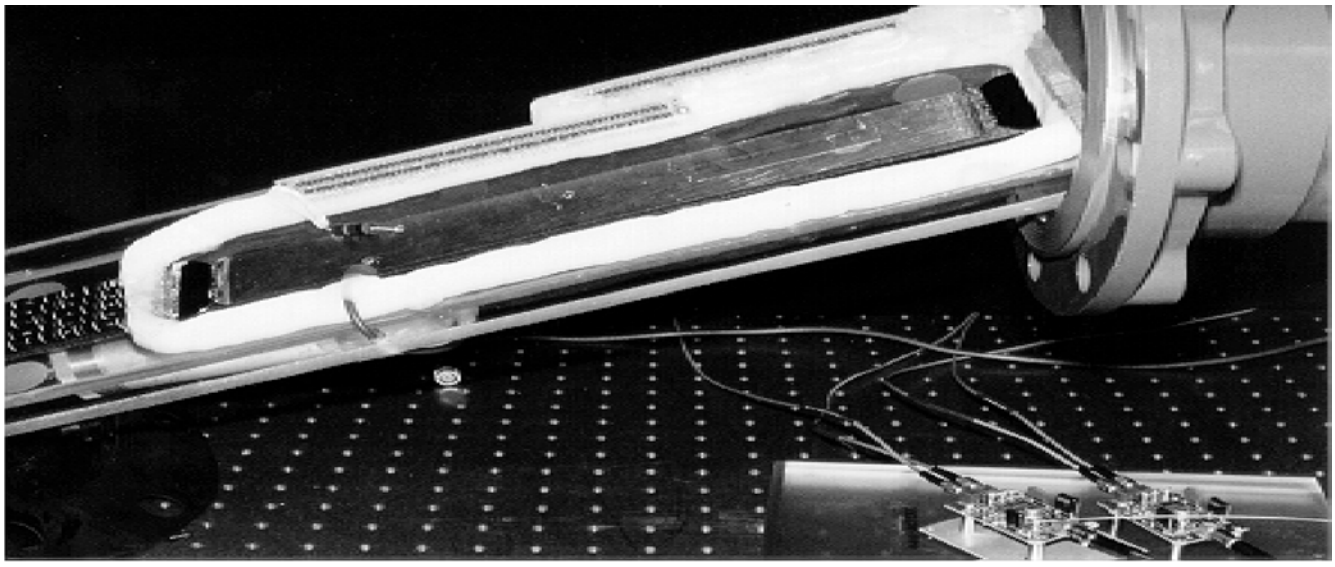

Figure 2.2-1 - Initial pulse forming line consisting of a length of transmission switched with PCSS at each end.

The development of the pulse forming line (PFL), which ultimately provides the transmitting antenna with the necessary waveform for GPR applications at Sandia, occurred over a period of 3 years. A simple PFL design consists of a single, 50-Ω transmission line switched at both ends with PCSS, shown in Figure 2.2-1.

By switching at each end of the transmission line, a single bipolar pulse could be formed (see Figure 2.2-2). Switch jitter was a major issue in reliable and consistent production of a bipolar pulse. This line was used for the initial GPR work reported in [4]. As PFL output was increased to produce higher levels of radiated electric fields, PCSS size increased, and so did jitter in the triggering of the two switches.

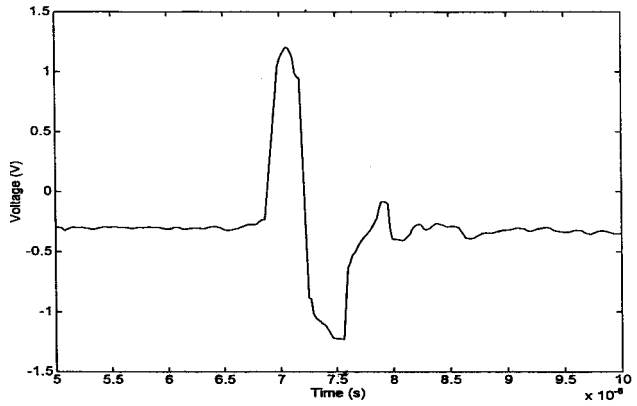

Figure 2.2-2 - Bipolar pulse produced by the 2-switch transmission line PFL.

2.2.2 FOLDED LINES

Eventually, the jitter in the 2-switch PFL becomes unacceptable (bipolar pulse generation unreliable) at higher voltages. Theoretically, this same transmission line could be folded back on itself and need only one switch to produce both halves of the bipolar pulse. The pulse produced from this folding is shown in Figure 2.2-3. The folded line delivers consistently a bipolar pulse with center frequency of approximately 140 MHz.

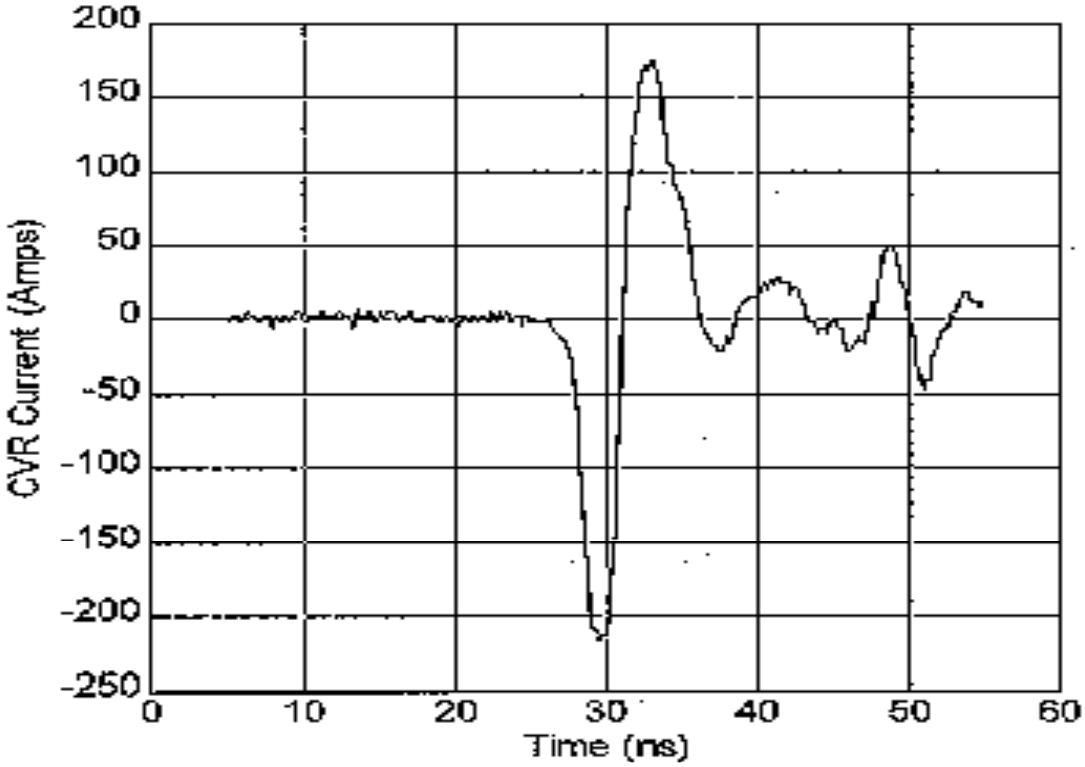

Figure 2.2-3 - Output pulse from the folded line PFL design. The measurement was made with a CVR at the end of a 50-Ohm transmission line.

2.2.3 FROZEN WAVE GENERATOR

The frozen wave generator (FWG) concept illustrated in Figure 2.2-4. The outer conductors of the two 50-Ω coaxial transmission lines are pulse-charged to ±V/2. Closing the center switch, PCSS, launches

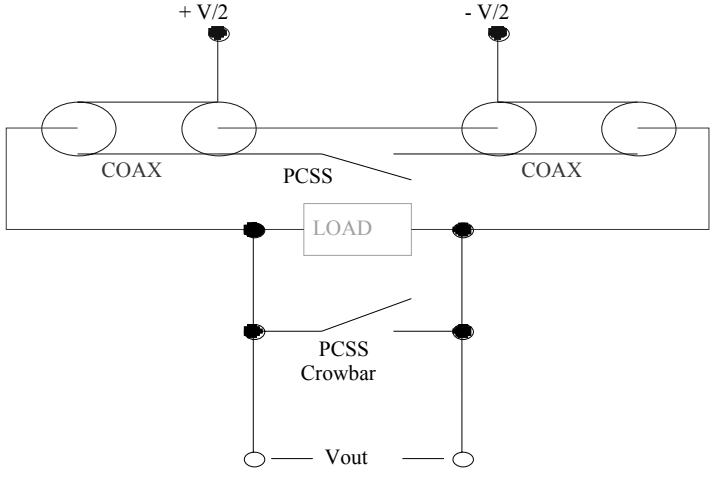

Figure 2.2-4- Drawing of the frozen wave generator concept.

a pulse in both directions out of each charged transmission line, which in turn add to ±V across the load (100 Ω) or antenna terminals. A crowbar switch was added to short out (crowbar) the forward going pulse after a single cycle to eliminate late time features for GPR applications.

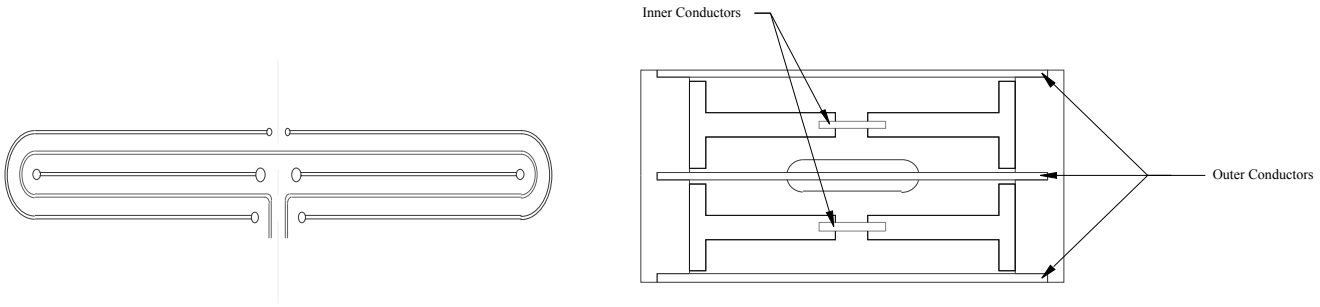

Figure 2.2-5 – Cutaway side (left) and end (right) views of the mechanical drawings of the rectangular coax FWG.

Instead of using a cylindrical coax, the conceptual design was folded back on itself and modified to a rectangular coaxial version. Views from the mechanical drawings of the field version of the FWG are shown in Figure 2.2-5.

Photographs of a rectangular coax FWG are shown in Figure 2.2-6. Visible in the photographs are the outer conductors in aluminum and brass, the series charging resistors, and the antenna terminals. The inner conductors and the PCSS main and crowbar switches can be seen in Figure 2.2-7.

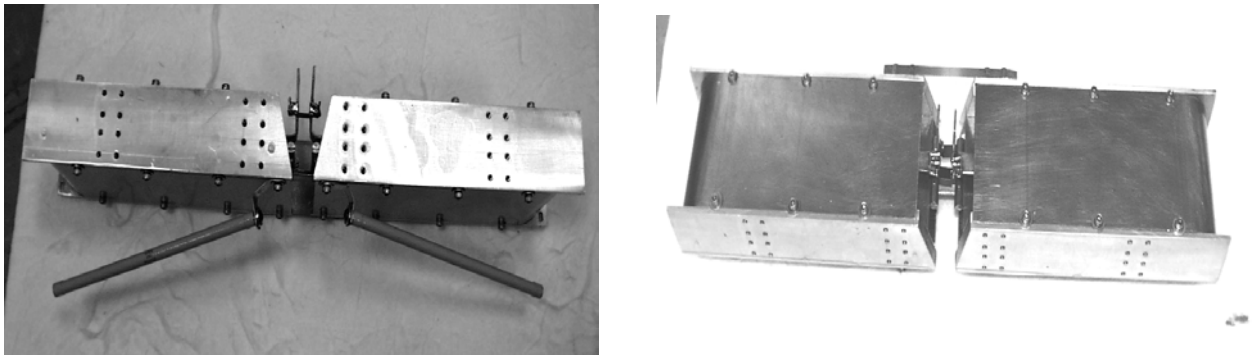

Figure 2.2-6 - Side (left) and bottom (right) views of the rectangular coax FWG. The housing measures 3-1/4 in. wide by 2 in. high by 16 in. long.

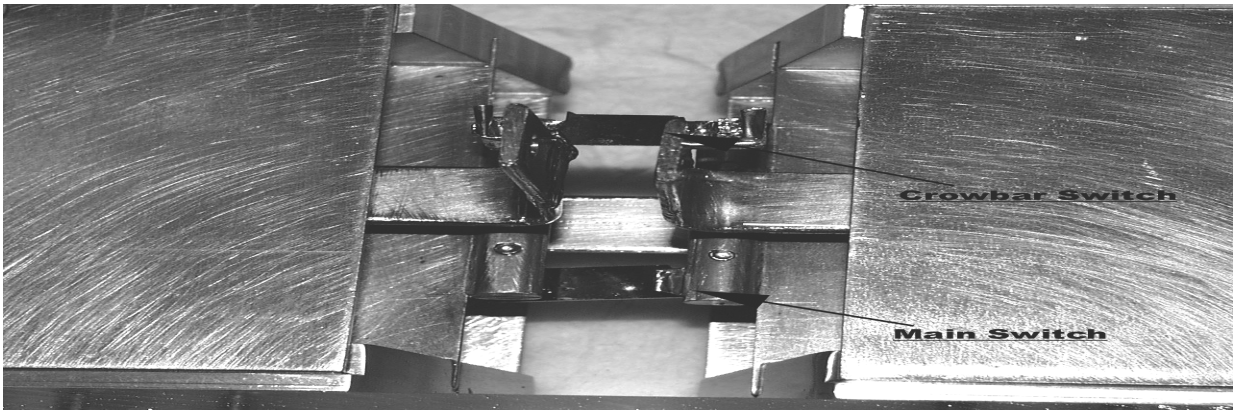

Figure 2.2-7 - Exposed center conductors, and main and crowbar PCSS.

The FWG was assembled as shown in Figure 2.2-8. The antenna terminals are in the foreground of the photograph. Connection to the charging resistors is achieved by the two white leads penetrating the back cover of the plastic box. When the FWG is running, the box is filled with silicone oil, which acts as the impedance-setting dielectric and high voltage insulation.

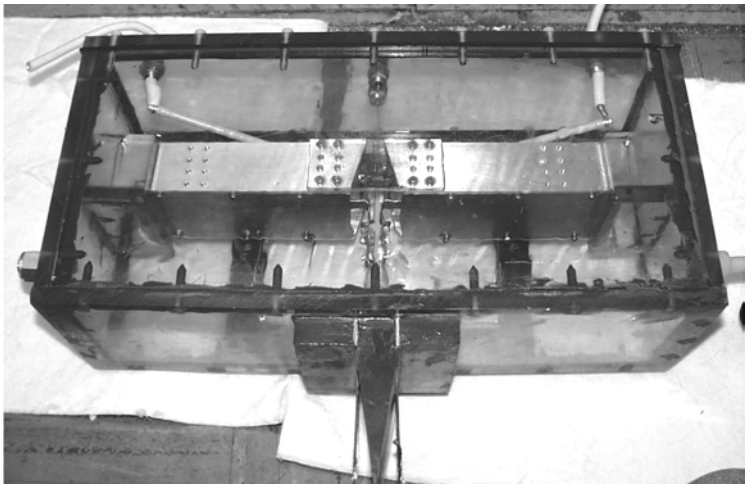

Figure 2.2-8 - FWG installed in its LEXAN box. 9 in. wide by 6-1/2 in. deep by 19 in. long.

Before the assembly was connected to an antenna, the antenna terminals were attached to a 100-Ω transmission line, which was terminated into a matched resistive load. When charged to ± 25 kV by the bipolar modulator, the output pulse, at the load, and its FFT, is shown in Figure 2.2-9. The output pulse measures 33 $kV_{peak\text{-}to\text{-}peak}$. Its frequency spectrum peaks at approximately 170 MHz, down ~5 dB at 250 MHz. Accounting for PCSS “lock-on” losses of about 4 kV/cm of switch gap length (8 kV total), the FWG is delivering ~80% of its charging voltage to the load.

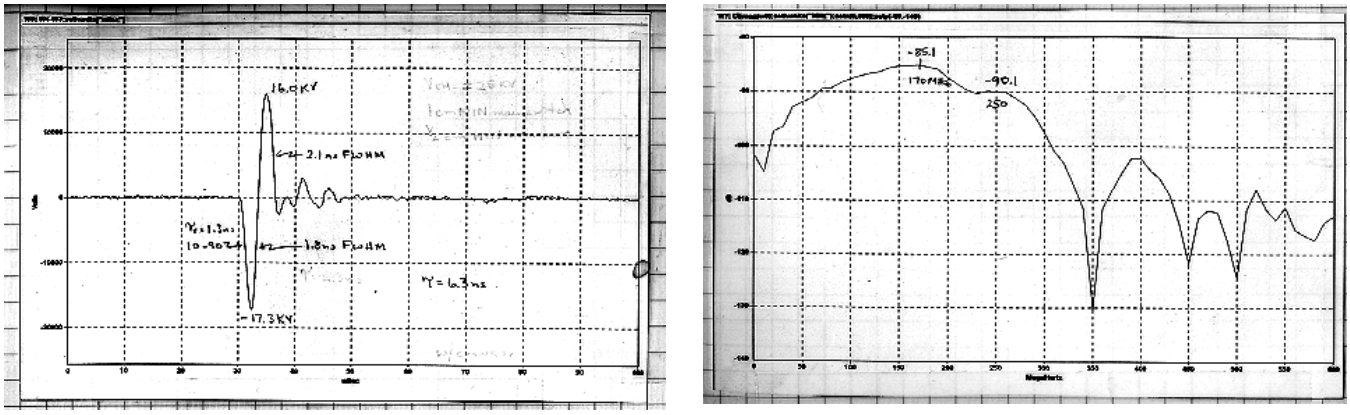

Figure 2.2-9 - FWG output pulse and its spectrum.

2.3 MODULATORS

Two different modulators are examined in this study. A dual-resonant modulator can be used to charge a variety of pulse forming lines that required a single polarity charge voltage. A different kind of modulator is necessary when bipolar charging is required.

2.3.1 DUAL-RESONANT MODULATOR

Figure 2.3.1-1 is a schematic of a modulator that can be used to charge double-switch and folded pulse-forming lines.

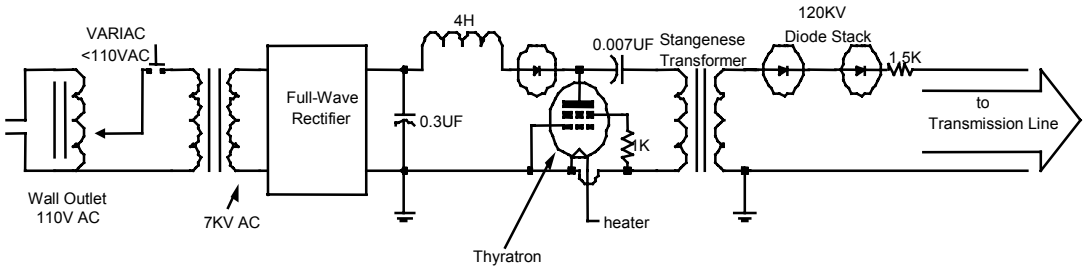

Figure 2.3.1-1 - Thyratron-based dual-resonant charging modulator.

AC supply voltage applied to the input of the modulator is stepped up, rectified, and in turn charges the 0.3 μF capacitor to V. When the thyratron switch closes, charge flowing from the capacitor through the

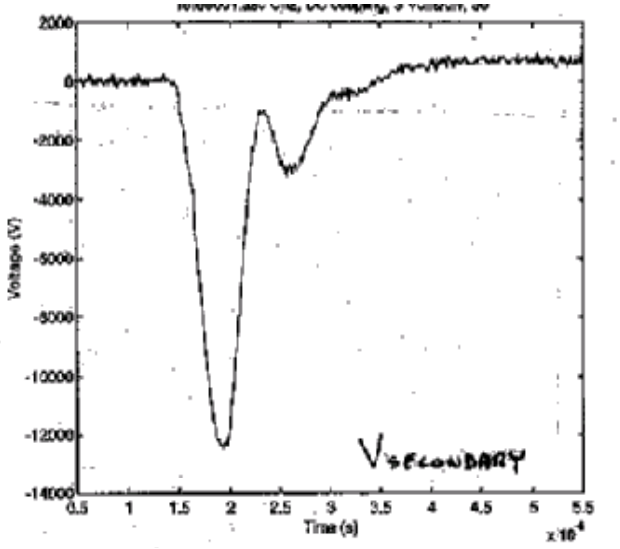

Figure 2.3.1-2 - Modulator output pulse at the secondary windings of the Stangenes transformer. Peak voltage is -12.5 kV.

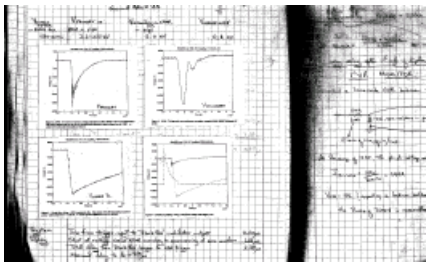

Figure 2.3.1-3 - Transmission line charging waveform after the diode stack. Peak voltage is 12 kV.

4 H inductor creates a magnetic field. The collapse of this field, when the thyratron opens, doubles the voltage across the 0.007 μF capacitor to 2 V—hence the name dual-resonant modulator. The output transformer has a primary to secondary windings ratio of 1:5.

The modulator's output pulse, measured at the secondary of the Stangenese transformer, shown in Figure 2.3.1-2, has a pulse width of ~1.5 μs FWHM. The short pulse width and single polarity voltage increase photoconductive semiconductor switch (PCSS) lifetime, which is a critical system parameter.

The charging waveform applied to the switched transmission lines, after the diode stack, is shown in Figure 2.3.1-3.

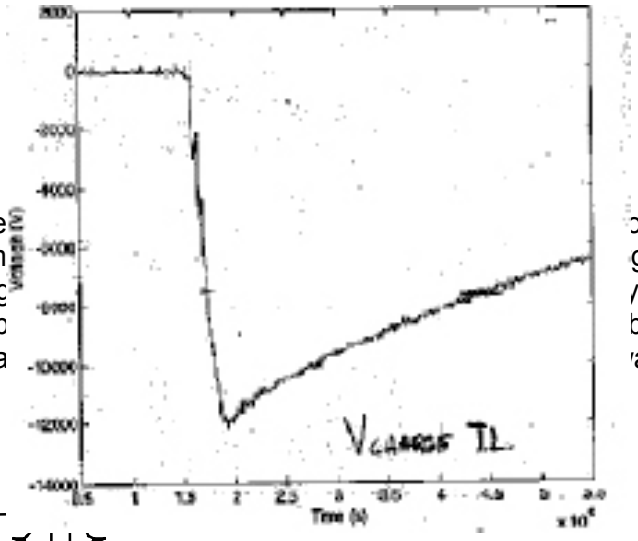

2.3.2 BIPOLAR MODULATOR

A frozen wave generator (FWG) design require output. Figure 2.3.2-1 is the schematic of the bipolar m ge the FWG. In this design, the primary energy storag ratron closes, the capacitor discharges through the p both a negative and positive output on the center-ta are is illustrated in Figure 2.3.2-2.

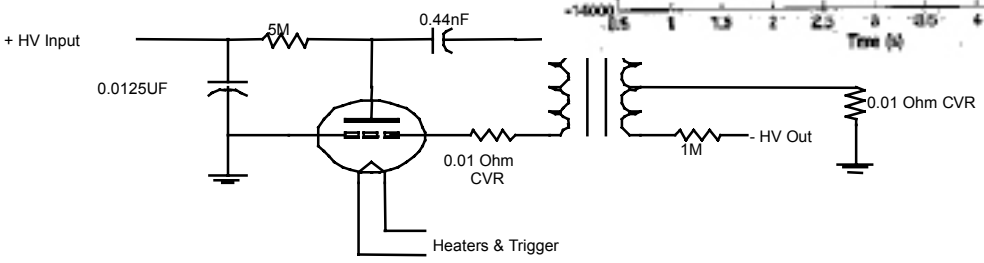

Figure 2.3.2-1 - Schematic of the bipolar modulator.

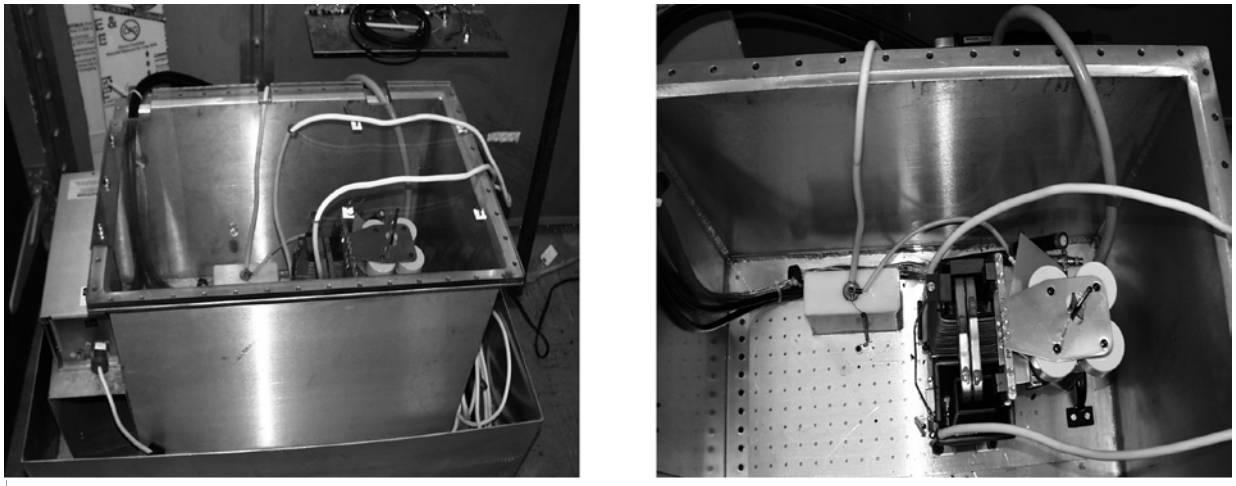

Figure 2.3.2-2 - Photographs of the bipolar modulator used to charge a frozen wave generator pulse forming line. The dimensions of the tank on the left are 18 in. wide by 18 in. high by 30 in. long.

The output pulse from this system was a factor of 5 shorter, approximately 250–300 ns FWHM, than the dual-resonant charging system; and therefore even more conducive to longer PCSS lifetime. It is also believed that a faster rising, shorter pulse may contribute to lower PCSS jitter. Figure 2.3.2-3 is an oscilloscope trace of the positive half of the modulator's output.

3. TRANSMIT ANTENNAS

The antenna type used for impulse systems has traditionally been the transverse electromagnetic (TEM) horn. Since the gain of an antenna depends on its size compared to the radiated wavelength, the size of a TEM horn is driven by the lowest significant frequency component in the impulsive waveform. As shown in Figure 3-1, these systems can be very large. The antenna shown is for a ground penetrating radar for which low frequency components down to around 70 MHz were important.

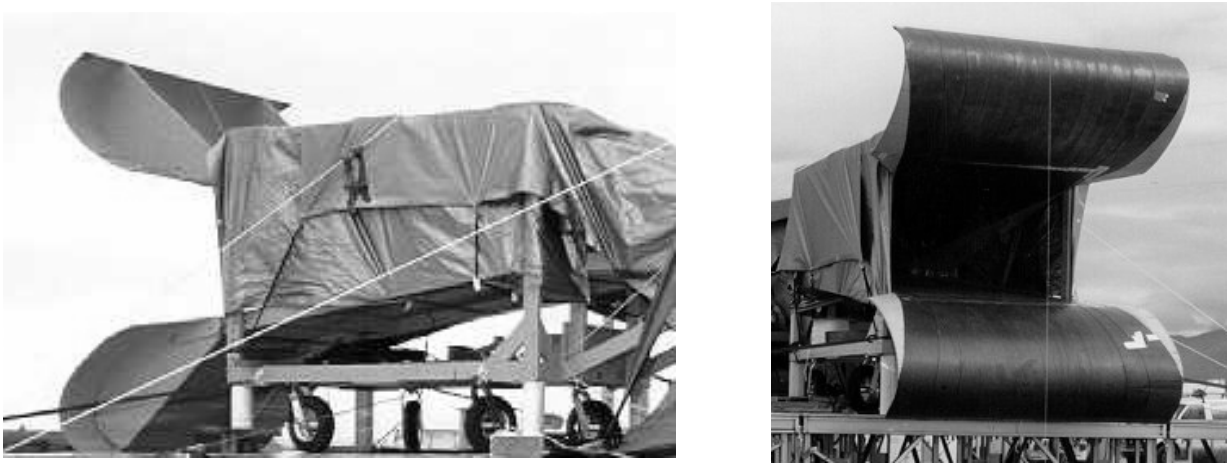

Figure 3-1 - Photographs of the transmit antenna used in the fall, '98, GPR outdoor test. The antenna measures 6 ft. wide by 7 ft. high by 14 ft. long, and it transmits frequency components to below 70 MHz.

TEM horns are very broadband and simply matched to the impulse transmitter by their smooth transitions in geometry. This comes at the cost of very large size. Other antenna types, however, can be used. For a compact system, small antennas need to be developed, which will have enough gain to generate sufficient field on target at an acceptable standoff, yet fit the form factor of the deployment vehicle. More highly resonant antennas distort the transient pulse shape, but this distortion may not be significant in terms of the impact on the target system. Very fat dipoles, for example, have been used in the VHF frequency range to transmit waveforms with 25% relative bandwidth. The dipoles were four inches in diameter and thirteen inches in length. The impulsive source was built inside. Such dipoles can be flattened into a “bow-tie” shape and made conformal with a platform surface. An antenna with these characteristics would turn an impulse into a damped ringing waveform of about four cycles at its natural resonant frequency. The gain of such an antenna is low. Larry Rinehart [5] provided some example data for such a radiator. Various fat dipoles of differing length-to-diameter (L/D) ratios were driven by a 700 MHz center-frequency LCO. Figure 3-2 illustrates his data for the peak field normalized to one-meter range. Fat dipoles (small L/D ratios) produce higher fields and shorter pulses. Thinner dipoles have lower fields but ring longer, concentrating their energy in a narrower frequency band.

A log-periodic antenna converts an impulse into a high-to-low frequency chirp. It can have slightly more gain than a dipole at the expense of this pulse distortion.

Compact antennas that transmit an acceptable pulse shape for the application while conforming to the platform constraints are clearly one of the greatest challenges to the design of usable systems.

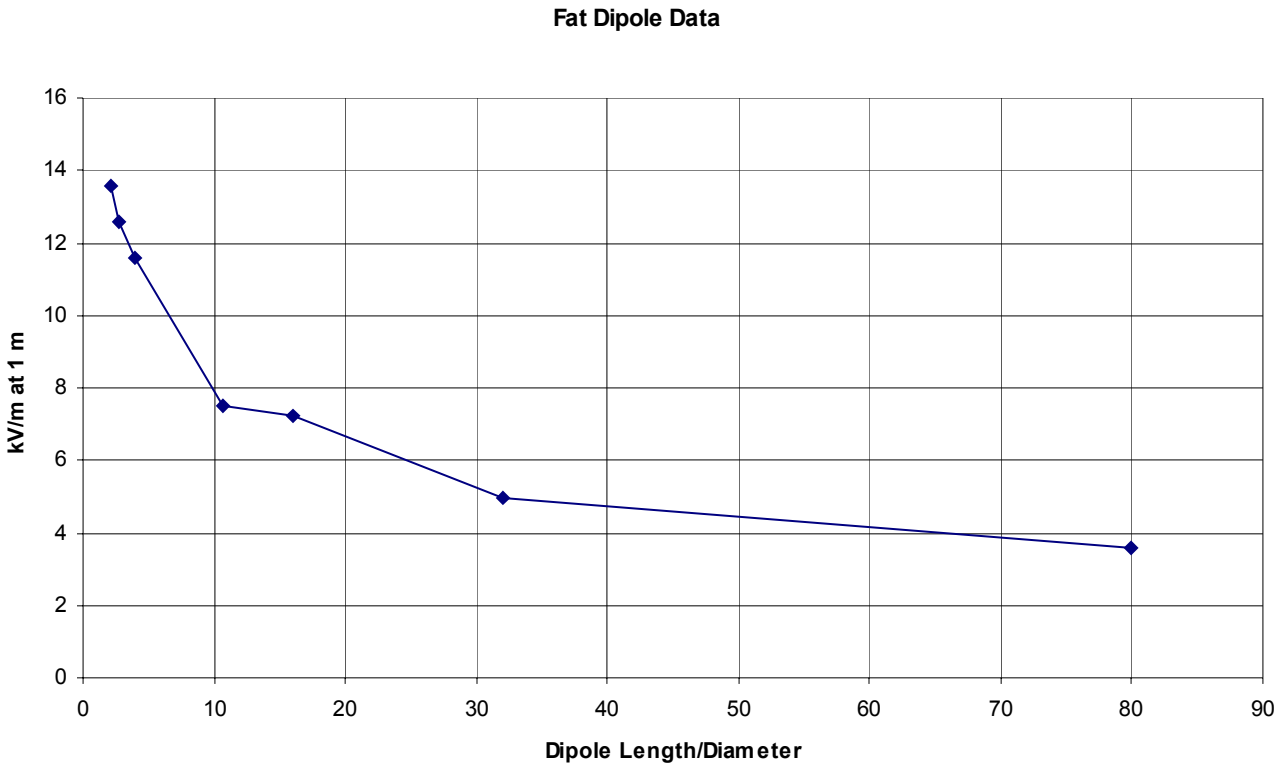

Figure 3-2 - Peak field vs L/D ratio

4. WEIGHT AND VOLUME CONSIDERATIONS

4.1 PCSS AND TRIGGER SOURCE

The PCSS device itself is very small and light, weighing about a gram and occupying less than 0.1 cc. The fiber-pigtailed diode laser arrays that are used to trigger the PCSS are also quite small and light, weighing perhaps 20 grams and occupying 2 cc. The avalanche transistor pulser circuit for the laser and its power supply could be laid out in a space of approximately 50 cc, on a circuit board of perhaps 5 x 3 cm, with a DC-DC converter to supply 400V that occupies less than 10 cc. With careful design, the PCSS and trigger source could be assembled to occupy less than 100 cc and weigh less than ~300 g.

4.2 LCO

This circuit requires relatively few elements, but requires layout dimensions for high voltage. On the order of 50 cc is probably necessary for this circuit, with the components weighing less than ~100 g.

4.3 FOLDED LINE-FROZEN WAVE GENERATOR

A folded transmission line topology takes considerable volume and weight. The frozen wave generator line occupies nearly 2000 cc. It is filled with dielectric fluid (silicone oil) for high voltage, and such fluids typically weigh ~1g/cc. Thus the weight will be dominated by the weight of dielectric fluid and is expected to be on the order of 2 kg.

4.4 MODULATORS

Advances in power electronics and high-voltage transformers have allowed compact, solid-state switching modulators to be built. As with the frozen-wave generator, the dielectric fluid, which can be used both for insulation and for cooling, will dominate the weight. The voltage required and the dielectric properties of the fluid drive the volume. If high average power is required instead of high peak power, thermal issues begin to drive the design.

4.5 ANTENNAS

As discussed in the previous section, the antenna is an integral part of both the impulse generator and the platform. Its largest dimension is driven by the wavelength of the lowest significant frequency component of the transmitted waveform. It is likely to be limited by platform size. It can be made from thin conducting sheet or film, however, so its weight is not a dominant issue. Good high-voltage engineering must be practiced, especially at the feed.

5. REFERENCES

[1] G. M. Loubriel et al, "Optically-Activated GaAs Switches For Ground Penetrating Radar And Firing Set Applications," *Proc. 12th IEEE Pulsed Power Conf.*, (IEEE, NY, 1999), Monterey, CA, 1999.

[2] G. M. Loubriel, M. W. O'Malley, and F. J. Zutavern, "Toward pulsed power uses for photoconductive semiconductor switches: closing switches," Proc. 6th IEEE Pulsed Power Conf., P. J. Turchi and B. H. Bernstein, eds., (IEEE, NY, 1987), Arlington, VA, June 29-July 1, 1987, pp. 145-148.

[3] R.L. Thornton, R.D. Burnham, T. L. Paoli, N. Holonyak Jr., and D. G. Deppe, “Optoelectronic device structures fabricated by impurity-induced disordering”, J. Crystal Growth 77, pp. 621-628, 1986.

[4] G. M. Loubriel et al. 1998. *Final Report of LDRD Project: Electromagnetic Impulse Radar for Detection of Underground Structures.* SAND98-0724. Sandia National Laboratories, Albuquerque, New Mexico.

[5] Larry Rinehart, Sandia National Laboratories. Private communication. May, 2002.

DISTRIBUTION

External Distribution:

20 Lockheed Martin Missiles and Fire Control–Dallas
Attn: Mark K. Browder, M/S: PT-88
P.O. Box 650003
Dallas, TX 75265-0003

Internal Distribution

1	MS	1165	William Guyton, 15300
1		1153	Malcolm Buttram, 15330-1
1		1153	Guillermo Loubriel, 15333
15		1153	Larry Bacon, 15333
5		1153	Alan Mar, 15333
1		1153	Larry Rinehart, 15333
1		1153	Robert Salazar, 15333
1		1153	Fred Zutavern, 15333
1		1153	Dale Coleman, 15336
1		1153	Steven Dron, 15336

1	MS	9018	Central Technical Files, 8945-1
2		0899	Technical Library, 9616
1		0612	Review & Approval Desk, 9612 For DOE/OSTI
1		0161	Patent and Licensing Office, 11500